Optimal Stent Implantation: Three-Dimensional Evaluation of the Mutual Position of Stent and Vessel Via Intracoronary Echocardiography

C Cañero[1], O Pujol[1], P Radeva[1], R Toledo[1], J Saludes[1], D Gil[1], JJ Villanueva[1], J Mauri[2], B Garcia[2], J Gomez[2], A Cequier[2], E Esplugas[2]

[1] Centre de Visió per Computador, Departament d'Informàtica UAB Bellaterra (Barcelona), Spain
[2] Departament d'Hemodinàmica, Hospital de Bellvitge (Barcelona), Spain

Abstract

We present a new automatic technique to visualize and quantify the mutual position between the stent and the vessel wall by considering their three-dimensional reconstruction.

Two deformable generalized cylinders adapt to the image features in all IVUS planes corresponding to the vessel wall and the stent in order to reconstruct the boundaries of the stent and the vessel in space. The image features that characterize the stent and the vessel wall are determined in terms of edge and ridge image detectors taking into account the gray level of the image pixels.

We show that the 3D reconstruction by deformable cylinders is accurate and robust due to the spatial data coherence in the considered volumetric IVUS image.

The main clinic utility of the stent and vessel reconstruction by deformable cylinders consists of its possibility to visualize and to assess the optimal stent introduction.

1. Introduction

Stents have become the most important advance in mechanical techniques for percutaneous coronary revascularization, since it is a minimum invasive technique to enlarge the vascular lumen, which decreases the risk of complications and restenosis. Nevertheless, after a successful operation, the patient could present an improper stent expansion. Is still unknown whether this occurs gradually or not.

IntraVascular UltraSound (IVUS) images provide a cross-sectional view of the vessel. Since it can be used both during and after the operation, a temporal pursuit of the stent expansion can be done.

Our aim is to obtain three-dimensional reconstruction of both the vessel and the stent from an IVUS volume in order to compute some measurements of their mutual position.

One-dimensional deformable models (snakes) are especially well suited for the problem of object recognition in medical imaging. However, the classical approach of segmenting 3-D images volumes slice by slice requires a post-processing to connect the sequence of 2-D contours into a continuous surface. Moreover, the resulting surface reconstruction could contain inconsistencies or show rings or bands.

The use of a true 3-D deformable surface model, on the other hand, can result in a faster, more robust segmentation technique that ensures a globally smooth and coherent surface between joining image slices.

In this paper, we propose the use of two deformable generalised cylinders that adapt to the image features in all IVUS planes corresponding to the vessel wall and the stent.

The article is organized as follows: int the next section we give a brief description of the two-dimensional deformable model used as well as the segmentation procedure. In section 3 we briefly discuss the applications of the 3D evaluation of the mutual position of the stent and the vessel wall. The paper finishes by presenting some conclusions and future research guidelines.

2. Two-dimensional deformable models

Due to the special skills of the B-Spline based deformable model [1], we have chosen it for our work.

A two dimensional deformable model is expressed as follows:

$$Q(u,v) = \sum_{i=1}^{M_u} \sum_{j=1}^{M_v} V_{ij} B_i(u) B_j(v)$$

Where V_{ij} is a set of control points, u, v the internal

Computers in Cardiology 1999;26:261-264.

parameters and $B_i(u)$, $B_j(v)$ are standard B-Spline blending functions[2].

Using Blake's notation[2], a B-spline sheet $\mathbf{Q}(u, v)$ of degrees d_u and d_v and $M_u \times M_v$ control points is defined parametrically for $0 \le u \le N_u$ and $0 \le u \le N_v$ as follows:

$$Q(u,v) = Q(s_u+\sigma_u, s_v+\sigma_v) = \left(1 \ \dots \ s_u^{d_u-1}\right) B_{\sigma_u} G_{\sigma_u} \mathbf{V} G_{\sigma_u}{}^T B_{\sigma_u}{}^T \begin{pmatrix} 1 \\ \vdots \\ s_v^{d_v-1} \end{pmatrix}$$

By using this expression, three simple topologies can be represented: planar, cylindrical and toroidal. Using aperiodic $B_i(u)$ and periodic $B_j(v)$ blending functions, we obtain a cylindrical topology for our model.

2.1. Internal energy

The deformable models are modeled to have restrictions to the stretching and bending of the model. An internal energy is associated to the model that decreases when the discontinuities of first and second degree reduce. With this purpose, two components of internal energy are defined by means of [3]:

Membrane energy given by the first derivative and keeps the continuity. For two-dimensional deformable models is given by:

$$E_{membrane}(Q) = \int \alpha_u \left(\frac{\partial Q}{\partial u}\right)^2 du + \int \alpha_v \left(\frac{\partial Q}{\partial v}\right)^2 dv$$

Thin-plate energy is computed from the second derivative and tries to keep a low curvature, avoiding the bending. In this case it is:

$$E_{thin-plate}(Q) = \int \beta_{uu}\left(\frac{\partial^2 Q}{\partial u^2}\right) + \beta_{uv}\left(\frac{\partial^2 Q}{\partial u \partial v}\right) + \beta_{vv}\left(\frac{\partial^2 Q}{\partial v^2}\right) du dv$$

A sum of *membrane energy* and *thin-plate energy* gives the internal energy:

$$E_{int}(Q) = E_{membrane}(Q) + E_{thin-plate}(Q)$$

For our deformable cylinder, the terms that affect the v parameter try to force the cross-area to be a little circle, whereas the terms that affect the u parameter preserve the coherence between planes. This fact gives robustness to our segmentation.

2.2. External energy

External energy is derived from the features of the images. By minimizing the external energy of the deformable model, external image forces help to push the shape towards the image features of interest.

Images are placed equally spaced along the z-axis, and control points are defined in order to make knots coincide with the image planes, as illustrated in figure 1.

Therefore, sampling in the u direction with step equal to the unity is enough to obtain the external forces.

Smoothing with a big gaussian and then applying a Haralick's edge detector we obtain a first approximation to the features corresponding to the vessel edges (see figure 2b).

Image ridges characterize the stent. We use the ridge detector defined by López et Al. in [4]. An example of this detection is shown in figure 2c.

Indeed, this feature extraction is not the best, and it is only a first approximation. Nevertheless, coherence between images and shape restrictions are taken into account by the internal energy of the deformable model. This fact allows us to deal with a poor segmentation.

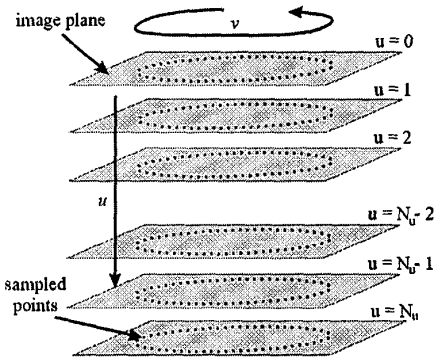

Figure 1. Control points are defined in order to make knots coincide with image planes.

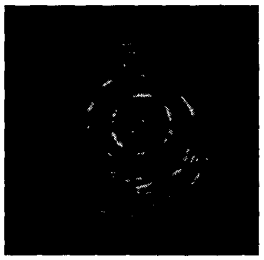

(a)

(b) (c)

Figure 2. Feature extraction from (a): The vessel wall is extracted via an edge detector (b) and ridges characterize the stent.

2.3. Energy minimization procedure

After this discussion, the basic problem is how to obtain the shape solution of the problem given an initial shape.

The most widely used way to minimize the energy was presented in [3] for one-dimensional snakes. This procedure is an *O(n)* iterative technique using sparse matrix methods, where *n* is the number of datapoints which conforms the deformable model.

For each iteration it take implicit Euler steps with respect to the internal energy and explicit Euler steps with respect to the external energy.

In fact, this procedure is an expression of $Q_t(u, v)$ in terms of $Q_{t-1}(u, v)$, where $Q_0(u, v)$ is the initial shape of the deformable model. More information about the minimization algorithm used can be found in [6].

The internal energy defined in 2.1 has a side effect of over-smoothing the shape during the energy minimizing process of the snake in absence of external forces. Since in this case the external forces are perpendicular to the z-axes, the knots will not coincide with the image planes after a deformation step. To cope with this problem, we deform only the *x* and *y* component of the cylinder (see figure 3).

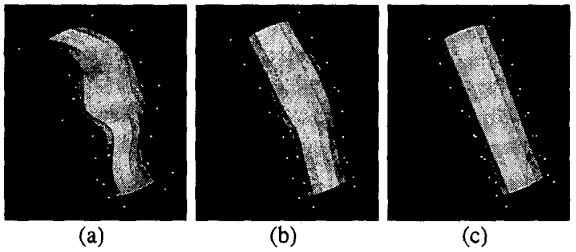

Figure 3. The terms of the internal energy that depend of *u* preserve the coherence between planes. (a) Original shape, (b) after 3 iterations and (c) after 20 iterations. Note that the length of the cylinder is not modified.

3. Application and visualization

Once the two cylinders have been adapted to the stent and to the vessel wall, the physician has a global view of its mutual position, as illustrated in figure 4. Note that this view provides a new perspective of IVUS imaging, since global qualitative information about the placement of the stent was not accessible before due to the local nature of the images.

Furthermore, since the shapes of the stent and the vessel wall are now available, several measurements can now be done in order to estimate the quality of the stent deployment by the IVUS criteria defined in [5], which have three parameters:

Cross-sectional area (CSA). The ratio of stent minimal CSA to normal reference vessel CSA (average CSA proximal and distal to stent) must be greater than 0.8.

Apposition. The maximum gap between the stent and the vessel wall must be not greater than 0.1mm.

Symmetry. The ratio of the stent minor axis to the stent major axis must be at less 0.7.

These concepts are illustrated in figure 5.

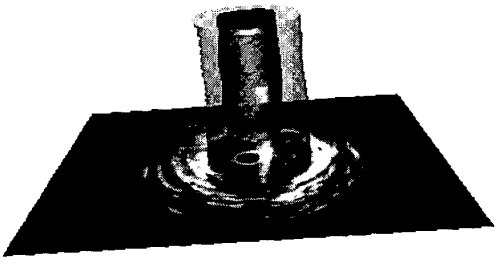

Figure 4. Global view of the mutual position of the stent and the vessel wall.

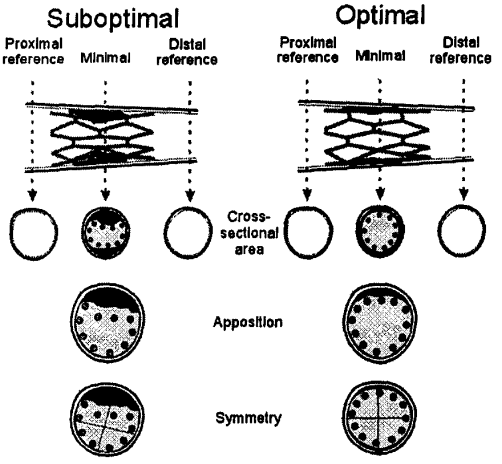

Figure 5. Optimal stent deployment: IVUS criteria[5].

These parameters are obtained plane by plane, and are accessible to the physician in terms of numerical data. In the case of the apposition, a color-coded distance map is offered in order of a more comprehensive interpretation of the stent deployment in the current plane (see figure 6); in this map, the color of each pixel indexes the minimum distance between the two shapes. The maximal value corresponds to the maximal gap.

Moreover, a temporal pursuit of the quality of the stent

deployment could be done, in order to study the evolution of the mutual position of stent and vessel wall, since it is still unknown whether improper stent expansion occurs gradually or not.

Furthermore, a quantitative assessment of the gain in lumen diameter after intervention can now be done.

Figure 6. Color-coded distance map of the mutual position of the stent and the vessel wall.

4. Conclusions

In this paper, we apply a deformable cylinder to segment and reconstruct the stent and the vessel wall from an IVUS images stack, instead of the classical approach of segmenting 3-D images volumes slice by slice.

The advantage of this approach is mainly the robustness that stems from the internal energy, which takes into account the coherence between image planes.

Since the feature extraction for the segmentation of the IVUS images is still an open problem, this fact is especially important, because the method gives encouraging results even from poorly segmented sequences.

However, our future research plans include the study and application of different feature extraction techniques, especially texture-based ones.

The 3D reconstruction obtained gives to the physician global qualitative information, but also quantitative for each slice. This information facilitates the diagnostic and pursuit of the patient.

Nevertheless, since after the deformation procedure we obtain the shape of both the stent and the vessel wall in terms of control points of a B-spline surface, this measurements could be taken analytically as done in [2], where re-parameterization invariant moments for closed curves in the plane are defined. By defining an analytical expression for the parameters of the IVUS criteria in terms of control points, we expect to obtain an accurate and efficient computation of the measurements.

Furthermore, we plan to fuse spatial information from automatic analysis of biplane angiograms [6] with structural information provided by intravascular ultrasound images. The main idea is to deform the cylinder following the path of the skeleton of the vessel reconstructed in 3D. This approach has two advantages: On the one hand, the internal energy takes into account that image planes are not parallel, and we expect that the results will improve due to the fact that the model is more approximated to the reality. On the other hand, the 3D reconstruction will be more realistic and will contribute to a better comprehension of the mutual position of the stent and the vessel wall by the physician. Work in this direction has been already done in [7], where the IVUS image plane are allocated in the three dimensional space and correctly oriented following the vessel skeleton path.

Acknowledgements

This work was supported by a research grant from CICYT with number TIC98-1100.

References

[1] Menet S, Saint-Marc P, Medioni G. B-snakes: Implementation and application to stereo. In: DARPA Image Understanding Workshop 1990. 259-268.

[2] Blake A, Isard M. Active Contours: the application of techniques from graphics, vision, control theory and statistics to visual tracking of shapes in motion. Springer-Verlag London Limited, 1998. 284-293.

[3] Kass M, Witkin A, Terzopoulos D. Snakes: Active contours using finite elements to control local shape. In: International Conference on Computer Vision 1987. 259-268.

[4] López A, Lumbreras F, Serrat J, Villanueva JJ. Evaluation of Methods for Ridge and Valley Detection. IEEE Transactions on Pattern Analysis and Machine Intelligence, 1999; 21(4):327-335.

[5] Robert D, Safian MD. Coronary Stents. In: The New Manual of Interventional Cardiology. Physician' Press, 1998:459:518.

[6] Cañero C, Deformable Models applied in Medical Imaging. Tech. report #33. Computer Vision Center. 1999.

[7] Pujol O, Model-Based 3D Interpolation of IVUS images. Tech. report #27. Computer Vision Center. 1999.

Address for correspondence:
Cristina Cañero
Computer Vision Center Edifici O Campus UAB
08193 Bellaterra (Cerdanyola) Barcelona, Spain
E-mail: cristina@cvc.uab.es